HHS Public Access

Author manuscript

Hear Res. Author manuscript; available in PMC 2019 June 01.

Published in final edited form as:

Hear Res. 2018 June ; 363: 109–118. doi:10.1016/j.heares.2018.03.012.

Effects of Cochlear Synaptopathy on Middle-Ear Muscle Reflexes in Unanesthetized Mice

M.D. Valero[1,2], **K.E. Hancock**[1,2], **S.F. Maison**[1,2], and **M.C. Liberman**[1,2]

[1]Eaton-Peabody Laboratories, Massachusetts Eye and Ear Infirmary, Boston, MA 02114, USA

[2]Department of Otolaryngology, Harvard Medical School, Boston, MA 02115, USA

Abstract

Cochlear synaptopathy, i.e. the loss of auditory-nerve connections with cochlear hair cells, is seen in aging, noise damage, and other types of acquired sensorineural hearing loss. Because the subset of auditory-nerve fibers with high thresholds and low spontaneous rates (SRs) is disproportionately affected, audiometric thresholds are relatively insensitive to this primary neural degeneration. Although, suprathreshold amplitudes of wave I of the auditory brainstem response (ABR) are attenuated in synaptopathic mice, there is not yet a robust diagnostic in humans. The middle-ear muscle reflex (MEMR) might be a sensitive metric (Valero et al., 2016), because low-SR fibers may be important drivers of the MEMR (Liberman and Kiang, 1984; Kobler et al., 1992). Here, to test the hypothesis that narrowband reflex elicitors can identify synaptopathic cochlear regions, we measured reflex growth functions in unanesthetized mice with varying degrees of noise-induced synaptopathy and in unexposed controls. To separate effects of the MEMR from those of the medial olivocochlear reflex, the other sound-evoked cochlear feedback loop, we used a mutant mouse strain with deletion of the acetylcholine receptor required for olivocochlear function. We demonstrate that the MEMR is normal when activated from non-synaptopathic cochlear regions and greatly weakened in synaptopathic regions and is a more sensitive indicator of moderate synaptopathy than the suprathreshold amplitude of ABR wave I.

Introduction

A principal pathology following many cochlear insults, including acoustic overexposure, is cochlear synaptopathy: the loss of synaptic connections between inner hair cells (IHCs) and auditory nerve fibers (ANFs). Acoustic overexposures causing only temporary threshold shifts can produce cochlear synaptopathy of as much as 50% without causing any loss of hair cells (Kujawa and Liberman, 2009), and IHCs surviving severe acoustic overexposures that cause permanent threshold shifts can lose as many as 80% of their afferent synapses (Valero et al., 2017). Furthermore, synaptopathy precedes hair-cell loss and permanent threshold elevation in aging mice (Fernandez et al., 2015), monkeys (Valero et al., 2017b), and humans (Viana et al., 2015). Because most ANFs contact a single IHC by a single synapse (Liberman, 1990), each missing synapse represents a silenced ANF, despite the fact

Corresponding author: Michelle D. Valero, 243 Charles St., Boston, MA 02114, Phone: (617) 573-5514, Fax: (617) 720-4408, michelle_valero@meei.harvard.edu.

that the cell body and central axon of the spiral ganglion neuron can survive for months or years (Johnsson, 1974; Felix et al., 2002; Kujawa and Liberman, 2009; Lin et al., 2011). The subset of ANFs with high thresholds and low or medium spontaneous-firing rates (low-SR fibers) appear to be most susceptible to damage by intense sound (Furman et al., 2013), aging (Schmeidt et al., 1996), and exposure to some ototoxic drugs (Bourien et al., 2014; Ruan et al., 2014). Because these fibers are unresponsive at low sound pressure levels, their loss is undetected by threshold measures (e.g., Furman et al., 2013). However, due to their high thresholds, low-SR fibers are crucial for encoding suprathreshold signals in background noise (Costalupes et al., 1984), and their loss may contribute to differences in speech-in-noise performance among aging and noise-exposed individuals (Alvord, 1983; Dubno et al., 1984; Rajan and Cainer, 2008; Kumar et al., 2012; Liberman et al., 2016).

Animal studies of noise-induced cochlear synaptopathy have shown that suprathreshold measures of cochlear neural function, such as wave-I amplitude of the auditory brainstem response (ABR), are progressively attenuated with increasing synaptic loss (e.g., Kujawa and Liberman, 2009; Lin et al., 2011), even after thresholds have recovered to normal. Correspondingly, speech-in-noise deficits in humans also correlate with suprathreshold electrophysiological measures that are consistent with the presence of synaptopathy (Liberman et al., 2016). However, because ABR wave I is dominated by onset responses, and low-SR fibers have relatively small onset responses compared to high-SR fibers (Versnel et al., 1990; Bourien et al., 2014), wave-I assays may not be the most sensitive measure of low-SR fiber loss.

The auditory periphery is endowed with a sound-evoked, negative-feedback reflex that innervates a striated muscle (the stapedius) connected to the stapes. When activated, this reflex reduces sound transmission through the middle ear. This middle-ear muscle reflex (MEMR) can be assayed non-invasively and can be part of a standard audiometric evaluation. It is commonly measured by monitoring the changes in sound pressure in the ear canal ipsilateral to a probe tone while eliciting the MEMR with a sound in either the ipsilateral or contralateral ear. The afferent limb of the MEMR circuit may be dominated by low-SR fibers (Liberman and Kiang, 1984; Kobler et al., 1992). If so, the MEMR should be especially sensitive to their loss in cochlear synaptopathy. Indeed, in anesthetized mice, the MEMR is permanently attenuated by noise-induced loss of IHC synapses, despite post-exposure recovery of ABR thresholds and little-to-no loss of hair cells (Valero et al., 2016).

However, because MEMR strength is attenuated by anesthesia (e.g., Borg and Moller, 1975; Valero et al., 2016; Xu et al., 2017), we developed an unanesthetized mouse preparation to provide a more realistic representation of normal MEMR function and the effects of noise-induced cochlear synaptopathy. To eliminate the possible confound from the medial olivocochlear (MOC) reflex, another sound-evoked negative-feedback reflex to the auditory periphery, we used a knockout mouse strain in which MOC efferent neurons are inactivated due to the absence of the α9 nicotinic acetylcholine receptor that is normally expressed on outer hair cells at MOC synapses (Vetter et al., 1999). Here, we show that our assay is specific to the MEMR and is sensitive to the degree of synaptic loss.

Methods

Animals and Groups.

CBA/CaJ;129S-Chrna9$^{tm1Bedv/J}$ mice were recovered from cryopreserved embryos at Jackson Laboratories and subsequently bred in-house. For noise exposure, unanesthetized α9 knockout (KO, N=6) and wild-type (WT, N=10) mice were placed inside a mesh cage atop a rotating platform within a reverberant chamber and exposed to octave-band noise (8–16 kHz) for 2 hrs at 93.5 dB SPL. One to two weeks later, cochlear function was measured (see below), and a head plate was surgically affixed to the skull. Following ≥ 48 hr recovery, MEMR growth functions were measured on 3 separate days prior to euthanasia. All metrics were compared against age-matched, unexposed controls (N=13 KO; N=4 WT). Mice with middle-ear problems, such as fluid behind the tympanic membrane or a collapsed pars flaccida, were excluded from the study, as were any mice with permanent threshold shifts following acoustic overexposure. An additional two KO mice were tested for the effects of anesthesia on the MEMR. To verify that MOC-mediated effects were absent in the KO mouse, shock-evoked DPOAE suppression was measured in one KO and one WT mouse with MEMs paralyzed by a systemic injection of curare, as in prior studies (e.g., Maison et al., 2007),. All procedures were approved by the Animal Care and Use Committee at the Massachusetts Eye and Ear Infirmary.

Cochlear Function Tests:

Mice were anesthetized with ketamine (100mg/kg) and xylazine (10mg/kg) and positioned on their side inside an electrically and acoustically shielded room maintained at 30°C. Booster injections (1/3 of the original dose) were given as needed, typically 45 minutes after the last injection.

For distortion-product otoacoustic emissions (DPOAEs), two primary tones, at frequencies f_1 and f_2 ($f_1<f_2$; $f_2/f_1=1.2$), were presented with L_1-L_2=10 dB. Stimulus duration was 300 ms at each increment of L_2 (10–80 dB SPL, 10-dB steps) at each f_2-frequency (5.6–45.2 kHz in ½ octave steps). DPOAE threshold was defined the L_2-level required to produce a DPOAE of 5 dB SPL. Primary tones were generated with 24-bit digital I-O cards (National Instruments PXI-4461) in a PXI-1042Q chassis, amplified by an SA-1 speaker driver (Tucker-Davis Technologies, Inc.), and delivered separately from two dynamic drivers (CUI CDMG15008–03A) in a custom acoustic system (http://www.masseyeandear.org/research/otolaryngology/investigators/laboratories/eaton-peabody-laboratories/epl-engineering-resources/epl-acoustic-system). An electret microphone (Knowles FG-23329-P07) at the end of a small probe tube in the acoustic system monitored ear-canal sound pressure levels.

Auditory brainstem responses (ABRs) were evoked with 5-msec tone pips (0.5-msec ramp, 40/sec, alternating polarity) at levels from 10–80 dB SPL and frequencies from 8–45.2 kHz (½-octave steps). ABRs were measured from transdermal electrodes in vertex-to-pinna configuration, with the ground placed just above the tail. 1024 artifact-free waveforms (512 of each polarity) were averaged at each frequency and level. A Grass pre-amplifier (Model P511) amplified (10,000X) and band-pass filtered (0.3–3 kHz) the ABR waveforms.

Threshold was defined by visual inspection of the stacked waveforms. Wave-I amplitude was defined as the difference between the first peak and the subsequent trough.

MEMR Measurements.

Mice were anesthetized briefly with 2% isoflurane. Plastic couplers, extending 7 mm from the microphone port of the acoustic systems, were secured in each ear canal with cyanoacrylate (VetBond®), and mice were secured by their head-plates atop a freely spinning disk on which they could walk at will. Once secured, isoflurane was removed, and mice were allowed to recover for 15 min prior to MEMR measurements. As schematized in Figure 1A, probe stimuli were 70–80 dB SPL, 2-msec Hanning-windowed "chirps," upswept from 4–32 kHz and presented at 40 Hz in two 11-sec 'trials.' As described previously (Valero et al., 2016), the phase spectrum was adjusted to compensate for the effect of the Hanning window, yielding a chirp with a flat magnitude spectrum (Neumann et al., 1994). Six seconds following the onset of the "chirp train," a reflex elicitor was presented contralaterally for 3 sec (100-msec rise-fall). Elicitors were spectrally flattened, audiometrically shaped, frozen noise of various bandwidths and incremented in level in 5-dB steps. On the second 11-sec trial, the elicitor was reversed in polarity to cancel any acoustic cross-talk in the final mean response waveform. A rotary encoder recorded the disk velocity, and chirps coinciding with a disk velocity ≥0.5cm/sec were rejected to exclude locomotion-related artifacts from analyses. The mean sound pressure waveform in the "probe ear" was computed by extracting the 2-ms segment of the microphone signal corresponding to each chirp (to exclude OAEs) and then averaging chirp by chirp across the two 11-sec trials. See text for further details.

Cochlear Immunostaining.

Mice were euthanized by transcardial perfusion while deeply anesthetized with ketamine. Following a 5-min perfusion with 4% paraformaldehyde, cochleas were exposed and perfused through the oval and round windows. Cochleas were then post-fixed for 2 hrs, decalcified in EDTA for 48 hrs at room temperature, and then dissected into half-turns and incubated in primary antibodies: 1) mouse (IgG1) anti-CtBP2 from BD Transduction Labs at 1:200; 2) mouse (IgG2) anti-GluA2 from Millipore at 1:2000, 3) rabbit αMyo7a from Proteus Biosciences at 1:200 for 18 hrs. Primary incubations were followed by two 1-hr incubations in species-appropriate secondary antibodies.

Innervation Analysis and Hair Cell Counts.

Cochlear lengths and a frequency-place map were obtained for each case from micrographs of dissected pieces using an imageJ plugin (http://www.masseyeandear.org/research/ent/eatonpeabody/epl-histology-resources/). Confocal z-stacks were collected using a 63x glycerol-immersion objective (N.A.=1.3) and 2.41X digital zoom on a Leica TCS SP8 confocal at cochlear frequency locations corresponding to the physiological assays. Synaptic ribbons (CtBP2-positive puncta) in the IHC area were counted using Amira (Visage Imaging), and the xyz coordinates were fed to custom re-projection software to assess the fraction of ribbons with closely apposed glutamate-receptor patches (i.e. GluA2 puncta) (Liberman et al., 2011).

Statistical Analyses.

Statistics were performed in Kaleidagraph (Synergy Software) and SPSS (IBM, v27). ANOVA and Wilcoxon-Mann-Whitney Rank Sum Tests, with Holm-Bonferoni corrections, were used to assess the significance of group differences.

Results

A. Measuring the wideband MEMR

High-level sounds can elicit bilateral contractions of the stapedius muscles in mammalian middle ears. These reflexive contractions increase the stiffness of the ossicular chain and thereby alter the reflection/absorption of sound waves at the eardrum (Geffcken, 1934). One method to estimate MEMR strength is by monitoring changes in the sound pressure level of an acoustic stimulus, or "probe," in one ear (i.e. the probe ear) while eliciting the reflex with sound presented to the contralateral ear (i.e. test ear), as illustrated in Figure 1A. The magnitude of the sound pressure changes (Δ dB) in the probe ear before vs. during the presentation of the contralateral elicitor is taken to represent the strength of the reflex. The Δ -dB spectra depend on frequency in a complicated, but reproducible, fashion (Fig. 1B), with only slight variations in the precise frequency locations of maxima and minima. An analysis window centered near 10 kHz reliably identifies a local minimum. In the unanesthetized mouse, the MEMR tends to increase in magnitude over the 3-sec presentation of the contralateral elicitor, particularly when elicited with low-level noise (see the orange and yellow traces in Fig. 1C, for 35- and 40-dB elicitors). We simplified group analyses by extracting a single metric to represent MEMR strength at each elicitor level. Our algorithm found the time window (including 3 consecutive time points) within the elicitor presentation in which the Δ dB was maximal.

The bandwidth and center frequency of the reflex elicitor determines the subset of ANFs in the "test ear" that drives the reflex. Broadband noise recruits fibers along the entire tonotopically organized cochlear spiral, while narrowing the noise band stimulates ANFs over a more limited cochlear span. The broadband and octave-band elicitors used here were audiometrically shaped, based on ANF data from mouse (Taberner and Liberman 2006), to compensate for differences in ANF threshold along the cochlear spiral, with the goal of recruiting similar functional subgroups (i.e. low- vs. high- SR fibers with high vs. low thresholds, respectively) with each increase in elicitor level. As shown in Figure 1D, the threshold for MEM contractions was 30–35 dB SPL for our broadband reflex elicitor, and the strength of the contractions increased monotonically over a wide range of elicitor levels.

B. Removing confounds of anesthesia and the medial olivocochlear system.

Contralateral-sound effects on ipsilateral auditory function can also be mediated by the medial olivocochlear reflex (MOCR) (Rasmussen 1946, 1953). The efferent limb of this bilateral, sound-evoked, negative-feedback loop consists of cholinergic neurons projecting to outer hair cells. When activated by sound, the MOCR decreases the contribution of outer hair cell electromotility to the amplification of sound-evoked cochlear vibrations, and can thereby modify otoacoustic emissions (OAEs) and/or ANF responses (Guinan, 2011). While the MOCR system cannot change middle-ear impedance, the MOCR could feasibly

attenuate ANF responses to the contralateral elicitor in the “test ear” and thereby reduce input to the MEMR circuit. To rule out potential contamination from the MOCR, we used a mutant mouse strain in which the MOC system is inactivated by targeted deletion of the specialized cholinergic receptor, α9, necessary for the peripheral effects of this pathway (Vetter et al., 1999). Because the MEMR involves neural circuitry in the brainstem and is subject to descending control from the cortex (e.g., Burns et al., 1993) and reticular formation (Borg, 1975; Joseph et al., 1985), it is modulated by the depth and nature of anesthesia (Borg and Moller, 1975; Valero et al., 2016; Xu et al., 2017). To assess the sensitivity of the MEMR to central anesthetics, MEMR growth functions were measured in α9 knockout mice before, during, and after anesthesia (Fig. 2). Isoflurane delivered at 2% quickly eliminated all signs of the MEMR (Fig. 2A). Under ketamine/xylazine anesthesia, MEMR threshold was elevated by ~56 dB by 11 mins post-induction, and the maximum strength (|Δ dB|, defined as the mean of the response to the two highest elicitor levels) was attenuated by 3 dB (Fig. 2B,C). The threshold and magnitude were stable at this weakened response strength for ~20 minutes and then slowly recovered to near-baseline values over the course of 90 minutes. Eighty minutes post-induction, the mouse was alert with a steady gait.

Aside from lacking a functional MOCR, α9 knockout (KO) mice were otherwise anatomically and functionally normal and similar to wild types (WTs). Afferent innervation density (Fig. 3A) and hair cell counts (Fig. 3D) were identical in KO and WT mice, as were thresholds for two measures of cochlear function (Fig. 3): 1) wave-I of the auditory brainstem response (ABR), which reflects the ensemble activity in ANFs (Buchwald and Huang, 1975; Antoli-Candela and Kiang, 1978) and 2) distortion product otoacoustic emissions (DPOAEs), a subtype of OAEs elicited by a pair of pure tones (Kim et al., 1980). To confirm the absence of MOCR function in KO mice, we paralyzed the middle ear muscles with a systemic injection of curare, and we monitored changes to DPOAEs while activating the MOC pathway with electric shocks at the floor of the IVth ventricle, as in prior studies (Maison et al., 2007). As expected, the robust MOC-mediated DPOAE suppression observed in WTs was absent in the KO (not shown).

MEMR thresholds and suprathreshold magnitudes were similar between KOs and WTs, when elicited by either octave-band (Fig. 4A-C) or broadband (Fig. 4D) stimuli, suggesting that our assay is dominated by the MEMR in mice. These data are consistent with our previous observation that middle-ear muscle paralysis fully eliminated the response in anesthetized mice (Valero et al., 2016). Furthermore, these data indicate that the assay retains its specificity for MEM-mediated effects even when MOC strength is increased by the lack of anesthesia (Chambers et al., 2013).

Given the lack of significant differences between effects in KOs and WTs, data were pooled across genotype for comparisons with noise-exposed mice.

C. MEMR strength in synaptopathic ears

Vulnerability to synaptopathy varies between species and mouse strains. In the mixed strain used here, octave-band noise (8–16 kHz) at 93.5 dB SPL presented for 2 hrs was sufficient to produce IHC synaptic loss (Fig. 5A) without significantly damaging OHCs (Fig. 5D) or permanently elevating ABR or DPOAE thresholds (Fig. 5B, E) in most mice. Because each

ANF contacts a single IHC via a single synaptic complex, the 40% loss of IHC synapses seen at the 32 kHz region, for example, represents the silencing of 40% of ANFs in that region. Thus, as seen previously in CBA/CaJ mice (e.g., Kujawa and Liberman, 2009) and guinea pigs (Furman et al., 2013), the mean suprathreshold amplitude of ABR wave-I was proportionately attenuated (~40%, on average) in synaptopathic regions with ~40% loss (Fig. 5C). Because most OHCs survived the noise exposure, threshold and suprathreshold DPOAEs were normal (Fig. 5E, F). In the mixed-strain used here, noise-induced synaptopathy was more variable than in CBA/CaJ, ranging from 4–50% in the 22–45 kHz region (Fig. 6B”, C”, red). The increased variability likely arises because CBA/CaJ are fully inbred, whereas the α9 line is non-congenic and therefore presents a genetic mixture of two contributing strains.

When MEMRs were elicited with octave-band noise centered on a low-frequency, non-neuropathic region (5.6–11.3 kHz), there was no significant effect of high-frequency synaptic loss in either MEMR threshold or maximum strength (Fig. 6A). When elicitor passband included the low-frequency edge of the synaptopathic region (11.3–22.6 kHz), the MEMR threshold was elevated (by 9.3 dB) and the maximum strength was attenuated (by 0.53 dB) relative to controls (Fig. 6A’). When the elicitor passband spanned the significantly synaptopathic region (22.6–45.2 kHz), MEMR threshold was more dramatically elevated (by 17.87 dB) and the maximum strength was significantly attenuated (by 0.66 dB) *re* controls (Fig. 6A”). In addition to octave-band elicitors, we used a broadband elicitor (4–64 kHz; Fig. 6A’’’-C’’’) to assay reflex strength across the whole tonotopic map. Here again, the reflex threshold was significantly elevated (by 6 dB) in synaptopathic mice, albeit to a lesser degree than with the high-frequency, octave-band elicitor. The largest decrement in maximum MEMR strength (0.73 dB) was observed with the broadband elicitor (Fig. 6A’’’,C’’’).

Because the noise produced a wide range of synaptopathy, we performed correlational analyses, as well (Fig. B-C’’’). The fractional synaptic loss within a frequency region was strongly correlated with both MEMR threshold and maximum strength: the correlation was strongest when the elicitor was filtered to stimulate the maximally synaptopathic region (Fig. 6A”-C”), or with a broad-band elicitor (Fig. 6B’’’-C’’’), and it was weakest in the non-synaptopathic region (Fig. 6B-C).

In addition, we assessed the sensitivity and specificity of the MEMR threshold within the maximally synaptopathic region (22–45 kHz) by measuring the area under a receiver-operating characteristic (ROC) curve. To establish the positive and negative groups in this continuous distribution of synapse survival, we used the 95% confidence interval (2-tail) around the mean of the unexposed controls (4.99% re mean). This was restrictive enough a cut-off to include some control animals in the ‘synaptopathic’ group. Even under these conditions, the area under the curve (AUC) was 0.938 (SE=0.0446), suggesting that the MEMR threshold would be ‘excellent’ at separating synapatopathic from non-synaptopathic ears. The caveat is that in humans the synaptopathic regions may not be as well-defined as in the mouse model of noise-induced synaptopathy. Furthermore, the mice included here represent a homogeneous population and in the clinic, there is a broader range of pathologies that could influence the metrics, including 8th nerve lesions and conductive hearing losses.

D. Comparison to other metrics of synaptopathy

Pearson correlation-coefficient matrices (Fig. 7) illustrate the relationships between each metric and synapse loss, using the MEMR elicitor passbands to bin the data. In the low-frequency, non-synaptopathic region (Fig. 7A), there was no significant relationship between the histological and physiological metrics. In the mildly synaptopathic region (11.3–22.6 kHz, Fig. 7B), where synaptopathy was ≤15% (see Fig. 6B'-C'), only the MEMR threshold was significantly correlated with the synaptic loss. The lack of correlation between ABR wave-I amplitude and moderate synapse loss is consistent with previous observations that wave I is insensitive to neural loss <20% (Bourien et al., 2014). OHC loss of ≤ 7% in this region was not captured by any physiological metric.

In the high-frequency region (22.6–45.2 kHz, Fig. 7C) synaptic loss was negatively correlated with both wave-I and MEMR amplitude and positively correlated with MEMR threshold. In this region, OHC loss of ≤ 9% was significantly correlated with MEMR threshold. However, OHC loss was also significantly correlated with synaptopathy, and there was no correlation between OHC loss and MEMR threshold after controlling for synaptopathy (r=0.22, p=0.32). When averaged across the length of the cochlea representing the broadband noise, including non-synaptopathic and synaptopathic regions, the percentage of synapses lost was ≤22% (see Fig. 6B"-C"). As was observed in the mildly synaptopathic, octave-band region, the MEMR metrics alone were significantly correlated with synapse loss (Fig. 7D).

Discussion

A. Specificity of the wideband reflex assay to the MEMR

Contributions of the MOC vs. MEM reflexes to sound pressure changes in the ear canal are notoriously difficult to disambiguate due to their overlapping dynamic ranges. Both reflexes can be elicited by a variety of moderate- to high-level sounds in either the ipsilateral or contralateral ears. The MEMR can alter ear-canal sound pressure of an ipsilateral probe stimulus by stiffening the ossicular chain and changing the absorbance/reflection of sound as it is transmitted through the middle ear. The MOC reflex can change ear-canal sound pressure by altering the levels of cochlear otoacoustic emissions (OAEs) via its action on the cochlear amplifier. When tonal probes are used, OAEs overlap with the probes in the time domain, and methods to separate MOCR vs. MEMR effects have been described elsewhere (Guinan et al., 2003; Sun, 2008). Because we used a stimulus transient (chirp) as our probe, we can separate MOC and MEM effects in the time domain. The timing between basally- and apically-driven nerve fiber responses, or the travelling-wave delay, in the mouse cochlea is ~1.6 msec (McGinley et al., 2012), so the time required for the chirp to propagate to the low-frequency OAE generation site in the cochlea, and for the OAE to propagate back through the middle ear to the ear canal is at least 2 msec. Thus, we recorded ear-canal sound pressure only during the presentation of the 2-msec chirps, and ignored the 23-msec inter-chirp interval during which the OAE contribution is expected. The effectiveness of this approach in minimizing the contributions of the MOCR is shown by the lack of difference in magnitude or threshold between wildtype mice and mutant mice with the MOCR inactivated by deletion of the α9 receptor. A similar paradigm recently applied to normal-hearing

humans also suggests that MEMR strength is estimable by monitoring changes to the sound pressure of transient stimuli, while MOCR strength is estimable by monitoring changes to the sound pressure of the delayed transient-evoked OAE (Marks and Seigel, 2017)

B. Sensitivity of the wideband MEMR to anesthesia and cochlear synaptopathy

The contralateral, sound-evoked MEM direct reflex arc is driven by auditory-nerve input to the ventral cochlear nucleus, which projects directly to stapedius motoneurons in the facial motor nucleus (Mukerji et al., 2010) and through an additional neuronal intermediary in the medial superior olive (reviewed by Moller, 1974; Borg and Moller, 1975). The MEMR is also subject to descending control from pathways that include the reticular formation (Borg, 1973; Joseph et al., 1985), the rubrobulbar tract (Courville, 1966; Borg, 1973b), the locus coeruleus, the inferior colliculus (Rouiller et al., 1989; Windsor et al., 2007), and the cortex (Baust and Berlucchi, 1964; Salomon, 1966; Burns, 1993). The sensitivity of the MEMR to anesthetics seen here and elsewhere (Fig. 2; Borg and Moller, 1975; Valero et al., 2016; Xu et al., 2017) may be partially attributable to a reduced excitability at neuromuscular junctions (Castro-Fonseca et al., 2015). However, an additional depressant effect on central circuitry or descending modulators is suggested by the observation that ipsilaterally evoked reflexes are less vulnerable to pentobarbital anesthesia than the more organizationally complex contralateral reflex (Borg and Moller, 1975).

The severity of MEMR deficits associated with synaptopathy appears to have been partially masked in our prior study by anesthesia-related elevations in baseline MEMR thresholds. In anesthetized mice with ~30% synapse loss, MEMR thresholds were elevated by ~6 dB in response to a high-pass elicitor spanning the synaptopathic region (Valero et al., 2016). Here, MEMR thresholds were elevated by ~15–17 dB in unanesthetized mice with the same degree of synaptopathy (Fig. 6B”). In the present study, elevations in MEMR thresholds scaled linearly with the percentage of synapses lost within the frequency region of the elicitor. The strength of the correlation between synapse loss and MEMR threshold and magnitude suggests that the noise-induced MEMR deficits reflect the silencing of ANFs that drive the reflex. An alternative hypothesis is that the acoustic overexposure could damage the stapedius motoneurons or the stapedius muscle itself. However, because the stapedius motoneurons are broadly tuned (Kobler et al., 1992), motoneuron or stapedius-muscle dysfunction should not cause frequency-dependent decrements in MEMR function, and therefore the MEMR elicited with low-frequency noise should also be attenuated for this to be true.

Prior neurophysiological studies in cat have suggested that the high-threshold, low-SR subset of ANFs might be especially important in driving the afferent loop of the MEMR (Kobler et al., 1992). This speculation was based on the observation that discharge rates in low-SR fibers show dramatic increases as sound pressure exceeds 80–90 dB SPL, which corresponds to the thresholds of stapedius motoneurons in the same type of barbiturate-anesthetized preparations (Kobler et al., 1992). These speculations, coupled with the observation that low-SR fibers are the most vulnerable to noise, suggested that the MEMR might be an especially sensitive metric of noise-induced synaptopathy. Because low-SR fibers constitute 40–50% of the ANF population in mice (Taberner and Liberman, 1996), the

synaptic losses of 40–50% observed in the present study might have eliminated all the low-SR fibers in the synaptopathic region. Although the MEMR thresholds were elevated by ~ 20 dB (e.g., Fig. 6), the reflex was not eliminated. This could be interpreted as evidence that both high- and low-SR fibers contribute to sensory drive for the MEMR. However, it is also possible low-SR ANFs from cochlear regions basal to the synaptopathic region (Fig. 5A) were recruited when stimulus levels were high enough to elicit a response from the low-frequency "tails" of their response areas. Future studies to produce broader regions of synaptopathy in the absence of hair-cell loss will help to clarify the hypothesis that low-SR fibers preferentially drive the reflex.

C. Potential consequences of MEMR dysfunction

One role of the MEMR is to protect the cochlea by reducing the input to the inner ear in high-noise environments (Borg et al., 1966; Brask, 1979). If the MEMR is weakened following noise-induced cochlear synaptopathy, then damaged ears could be rendered more vulnerable to subsequent noise exposures. Indeed, a single exposure to 100-dB SPL noise causes only temporary threshold shifts and permanent cochlear synaptopathy in CBA/CaJ mice, but 3 exposures at the same level cause permanent threshold shifts and irreversible hair-cell loss in the high-frequency, basal half of the cochlea that resembles the pattern of age-related hearing loss (Wang and Ren, 2012). If it is true in humans that the MEMR is weakened in cochlear synaptopathy, then early identification and enhanced protective measures or treatment may be key to minimizing further damage. Indeed, prior to OSHA regulations that limit exposures to 85 dB SPL or lower within an 8-hr workday, industrial workers were exposed to high-noise levels that were sufficient to cause TTS. Over time, daily exposures to noise levels that initially produced only TTS resulted in a progression to PTS (Passchier-Vermeer, 1974). Given the current data, it is tempting to speculate that the progression occurred, at least in part, due to the deterioration of the protective MEMR.

MEMRs were elicited here with broadband stimuli as low-level as ~35 dB SPL, and human MEMRs have been elicited at levels near 50–60 dB SPL (van de Berge, 1990; Guinan et al., 2003; Goodman and Keefe, 2006; Zhao and Dhar, 2010), neither of which are considered to be damaging noise levels against which an ear needs to be protected. Another important role of the MEMR is to reduce the masking of high-frequency signals by low-frequency noise, i.e. reduce the upward spread of masking (Pang and Guinan, 1997). This may explain why humans that are unilaterally areflexive due to Bell's palsy (Borg and Zakrisson, 1973, 1974; McCandless and Schumacher, 1979), a condition in which unilateral facial-nerve paralysis disables the MEMR on that side, or due to stapedectomy (Liden et al., 1963; Chadwell & Greenberg, 1979; Colletti et al., 1988), have difficulty interpreting high-level speech and speech-in-noise when tested in the affected ear. It has been argued that ANF dysfunction is a potential comorbidity in Bell's palsy (see Phillips et al., 2002), and that either pathology could explain these behavioral deficits. Nonetheless, physiological data in cats demonstrate a clear role of the MEMR in unmasking (Pang and Guinan, 1997). Future studies should attempt to disambiguate the contribution of ANF dysfunction and MEMR dysfunction to hearing-in-noise and speech-intelligibility deficits.

D. The clinical utility of the MEMR in diagnosing cochlear synaptopathy

In the clinic, MEMRs are often measured from adults in conjunction with tympanometry, in which the static ear-canal pressure is varied to find maximal reflectance of a 226 Hz probe tone, and a reflex elicitor is played either ipsilaterally or contralaterally while the canal is held at that pressure. MEMR thresholds in normal-hearing listeners are usually ≥ 70 dB SPL when elicitors are 0.5, 1, 2, or 4 kHz tones, or broadband noise (Feeney and Keefe, 2001). This type of MEMR assay has aided in screening for facial nerve dysfunction, conductive hearing loss, including otosclerosis, and has also been valuable in the diagnoses of severe auditory neuropathy, including auditory nerve tumors (Anderson et al., 1970; reviewed by Schairer et al., 2007). However, if MEMR thresholds measured from 'normal' ears are so high, and because high-level reflex elicitors can cause cochlear damage (see Schairer et al., 2013), a ceiling effect can limit the usefulness of this assay. Indeed, in cases of auditory-nerve tumors and severe auditory neuropathy, the MEMR threshold is often immeasurable in this way. Even when nerve function is sufficient to elicit a reflex, it decays rapidly when compared with 'normal' ears (Anderson et al., 1970; Cartwright and Lilly, 1976; Silman et al., 1978; see Wilson et al., 1984; Berlin et al., 2005, 2010).

Replacing the 226 Hz probe tone with a click or a chirp, as we did in the present study, allows for the analysis of MEMR-effects over a wider range of frequencies, and in humans, wideband-MEMR thresholds are up to 24 dB lower than standard MEMR thresholds (Feeney and Keefe 2001; Feeney et al., 2017). Recent efforts by Feeney, Keefe, et al. (2017) to establish normative wideband reflex parameters will advance the clinical utility of this assay. As for the standard MEMR assay described above, the wideband reflex will likely be sensitive to a variety of otologic disorders, limiting its diagnostic *specificity*. However, the findings reported here suggest that the MEMR may be a useful tool in a diagnostic battery of tests designed to identify cochlear synaptopathy in humans, particularly because the test can be finished within a few minutes. The data here suggest that if conductive hearing loss can be ruled out, then the reflex threshold may be able to identify narrowband regions of synaptopathy with octave-band resolution and estimate the severity of the pathology.

Acknowledgements

We thank the lab of Daniel Polley for advice in the construction of the rotary wheel for unanesthetized recordings. We thank John Guinan for helpful discussions. Research supported by grants from the National Institute on Deafness and other Communication Disorders: F32 DC 014405 (MDV) and R01 DC 00188 (MCL).

REFERENCES

Alvord LS (1983). Cochlear dysfunction in "normal hearing" patients with history of noise exposure. Ear and Hearing, 4, 247–250. [PubMed: 6628849]

Anderson H, Barr B, Wedenberg E (1970). The early detection of acoustic tumours by the stapedius reflex test In: Sensorineural Hearing Loss, pp. 275–294. Editors: Wolstenholme GEW and Knight J. J. and A. Churchill London.

Antoli-Candela F, Jr., Kiang NYS (1978). Unit activity underlying the N1 potential In: Evoked electrical activity in the auditory nervous system (Naunton RF, Fernandez C, eds), pp 165–191. New York: Academic.

Baust W, Berlucchi G, Moruzzi C (1964). Change in the auditory input during arousal in cats with tenotomised middle ear muscles. Archives Italiennes de Biologie, 102, 675–85. [PubMed: 14230776]

Berlin CI, Hood LJ, Morlet T, Wilensky D, Mattingly KR, Taylor-Jeanfreau J, Keats BJB, St. John P, Montgomery E, Shallop JK, Russell BA, Frisch SA (2010). Multi-site diagnosis and management of 260 patients with auditory neuropathy/dys-synchrony (auditory neuropathy spectrum disorder*). Int. J. Audiol 49, 30–43. [PubMed: 20053155]

Berlin CI, Hood LJ, Morlet T, Wilensky D, St. John P, Montgomery E, Thibodaux M (2005). Absent or elevated middle ear muscle reflexes in the presence of normal otoacoustic emissions: a universal finding in 136 cases of auditory neuropathy/dys-synchrony. J. Am. Acad. Audiol 16, 546–53. [PubMed: 16295241]

Borg E (1966). A quantitative study of the effect of the acoustic stapedius reflex on sound transmission through the middle ear of man. Acta-Otolaryngol. 66, 461–72.

Borg E (1973). On the neuronal organization of the acoustic middle ear reflex: A physiological and anatomical study. Brain Research, 49, 101–23. [PubMed: 4349006]

Borg E, and Møller AR (1975). Effect of central depressants on the acoustic middle ear muscle reflex in rabbit. Acta Physiol. Scand. 94, 327–38. [PubMed: 1180078]

Bourien J, Tang Y, Batrel C, Huet A, Lenoir M, Ladrech S, Desmadryl G, Nouvian R, Puel J, Wang J (2014). Contribution of auditory nerve fibers to compound action potential of the auditory nerve. J. Neurophysiol 112, 1025–39. [PubMed: 24848461]

Brask T (1979). The noise protection effect of the stapedius reflex. Acta. Otolaryngol. Suppl. 330, 116–7.

Brownell WE, Bader CR, Bertrand D, Ribaupierre YD (1985). Evoked mechanical responses of isolated cochlear outer hair cells. Science. 227, 19–46.

Buchwald JS, Huang C (1975). Far-field acoustic response: origins in the cat. Science 189:382–384. [PubMed: 1145206]

Burns EM, Harrison WA, Bulen JC, Keefe DH (1993). Voluntary contraction of middle ear muscles: effects on input impedance, energy reflectance and spontaneous otoacoustic emissions. Hear Res 67:117–127. [PubMed: 8340262]

Cartwright D, and Lilly D (1976). A comparison of acoustic reflex decay patterns for patients with cochlear and VIIIth-nerve disease American Speech-Language-Hearing Association Convention. Houston

Chadwell DL, and Greenberg HJ (1979). Speech intelligibility in stapedectomized individuals. Am. J. Otol 1, 103–8. [PubMed: 554471]

Chambers AR, Hancock KE, Maison SF, Liberman MC, Polley DB (2012). Sound-evoked olivocochlear activation in unanesthetized mice. J. Assoc. Res. Otolaryngol 13, 209–17. [PubMed: 22160753]

Colletti V, Sittoni V Fiorino FG (1988). Stapedotomy with and without stapedius tendon preservation vs stapedectomy long-term results. Am. J. Otol 9, 136–41. [PubMed: 3407746]

Costalupes JA, Young ED, Gibson DJ (1984). Effects of continuous noise backgrounds on rate response of auditory nerve fibers in cat. J. Neurophysiol 51, 1326–44. [PubMed: 6737033]

Courville J (1966). Rubrobulbar fibers to the facial nucleus and the lateral reticular nucleus (nucleus of the lateral funiculus). An experimental study in the cat with silver impregnation methods. Brain Res., 1, 317–337. [PubMed: 4164099]

Dubno JR, Dirks DD, Morgan DE (1984). Effects of age and mild hearing loss on speech recognition in noise. J. Acoust. Soc. Am, 76, 87–96. [PubMed: 6747116]

Feeney MP, and Keefe DH (2001). Estimating the acoustic reflex threshold from wideband measures of reflectance, admittance, and power. Ear Hear. 22, 316–32. [PubMed: 11527038]

Feeney MP, Keefe DH, Hunter LL, Fitzpatrick DF, Garinis AC, Putterman DB, McMillan GP (2017). Normative wideband reflectance, equivalent admittance at the tympanic membrane, and acoustic stapedius reflex threshold in adults. Ear Hear. 38, 142–60.

Felix H, Pollak A, Gleeson M, Johnsson LG (2002). Degeneration pattern of human first-order cochlear neurons. Adv Otorhinolaryngol. 59 116–23 [PubMed: 11885652]

Fernandez KA, Jeffers PW, Lall K, Liberman MC, Kujawa SG. (2015). Aging after noise exposure: acceleration of cochlear synaptopathy in “recovered” ears. J. Neurosci 13, 7509–20.

Furman AC, Kujawa SG, Liberman MC (2013). Noise-induced cochlear neuropathy is selective for fibers with low spontaneous rates. J. Neurosci 110, 577–86.

Goodman SS, and Keefe DH (2006). Simultaneous measurement of noise-activated middle-ear muscle reflex and stimulus frequency otoacoustic emissions. J. Assoc. Res. Otolaryngol 7, 125–39. [PubMed: 16568366]

Goodman SS, Fitzpatrick DF, Ellison JC, Jesteadt W, Keefe DH (2009). High-frequency click-evoked otoacoustic emissions and behavioral thresholds in humans. J. Acoust. Soc. Am 125, 1014–32. [PubMed: 19206876]

Guinan JJ, Backus BC, Lilaonitkul W, Aharonson V (2003). Medial olivocochlear efferent reflex in humans. Otoacoustic emission (OAE) measurement issues and the advantages of stimulus frequency OAEs. J. Assoc. Res. Otolaryngol 4, 521–40 [PubMed: 12799992]

Guinan JJ (2011). Physiology of the medial and lateral olivocochlear systems In: Auditory and Vestibular Efferents (Eds. Ryugo DK, Fay RR, and Popper AN).

Johnsson L (1974). Sequence of degeneration of Corti's organ and its first-order neurons. Ann. Otol. Rhinol. Laryngol 83, 294–303. [PubMed: 4829736]

Joseph MP, Guinan JJ, Jr, Fullerton BC, Norris BE, Kiang NY (1985). Number and distribution of stapedius motoneurons in cats. Journal of Comparative Neurology, 232, 43–54. [PubMed: 3973082]

Kemp D (1978). Stimulated acoustic emissions from within the human auditory system. J. Acoust. Soc. Am 64, 1386–91. [PubMed: 744838]

Kim DO, Molnar CE, Matthews JW (1980). Cochlear mechanics: Nonlinear behavior in two-tone responses as reflected in cochlear-nerve-fiber responses and in ear-canal sound pressure. J Acoust Soc Am. 67, 1704–21 [PubMed: 7372925]

Kobler JB, Guinan JJ, Jr., Vacher SR, Norris BE (1992). Acoustic reflex frequency selectivity in single stapedius motoneurons of the cat. J. Neurophysiol 68, 807–17. [PubMed: 1432049]

Kujawa SG, and Liberman MC (2009). Adding insult to injury: cochlear nerve degeneration after "temporary" noise-induced hearing loss. J. Neurosci 29, 14077–85. [PubMed: 19906956]

Kumar UA, Ameenudin S, Sangamanatha AV (2012). Temporal and speech processing skills in normal hearing individuals exposed to occupational noise. Noise and Health, 14, 100–5. [PubMed: 22718107]

Liberman LD, Wang H, Liberman MC (2011). Opposing gradients of ribbon size and AMPA receptor expression underlie sensitivity differences among cochlear-nerve/hair-cell synapses. J. Neurosci 31, 801–8. [PubMed: 21248103]

Liberman MC (1990). Afferent and efferent innervation of the cat cochlea: quantitative analysis with light and electron microscopy. J Comp Neurol. 301, 443–60. [PubMed: 2262601]

Liberman MC, Epstein MJ, Cleveland SS, Wang H, Maison SF (2016). Toward a differential diagnosis of hidden hearing loss in humans. PLoS One. 2016 11, e0162726. [PubMed: 27618300]

Liberman MC, and Kiang NYS (1984). Single-neuron labeling and chronic pathology. IV. Stereocilia damage and alterations in rate and phase level functions. Hear. Res 16, 75–90. [PubMed: 6511674]

Liden G, Nordlund B, Hawkins JE, Jr. (1964). Significance of the stapedius reflex for the understanding of speech. Acta Otolaryngol. Suppl 188(S), 275

Lin HW, Furman AC, Kujawa SG, Liberman MC (2011). Primary neural degeneration in the guinea pig cochlea after reversible noise-induced threshold shift. J. Assoc. Res. Otolaryngol 12, 605–16. [PubMed: 21688060]

Maison SF, Vetter DE, Liberman MC (2007). A novel effect of cochlear efferents: in vivo enhancement does not require a9 cholinergic receptors.

Marks KL, and Siegel JH (2017). Differentiating middle ear and medial olivocochlear effects on transient-evoked otoacoustic emissions. J. Assoc. Res. Otolaryngol 18, 529–42. [PubMed: 28432471]

McGinley M, Liberman MC, Bal R, Oertel D (2012). Generating synchrony from the asynchronous: compensation for cochlear traveling wave delays by the dendrites of individual brainstem neurons. J. Neurosci 32, 9301–11. [PubMed: 22764237]

Møller AR (1984). Neurophysiological basis of the acoustic middle-ear reflex In: The Acoustic Reflex (Ed. Silman Shlomo). Academic Pres, Inc.

Mukerji S Windsor AM, Lee DJ (2010). Auditory brainstem circuits that mediate the middle ear muscle reflex. Trends Amplif. 14, 170–91. [PubMed: 20870664]

Neumann J, Uppenkamp S, Kollmeier B (1994). Chirp evoked otoacoustic emissions. Hear. Res. 79, 17–25. [PubMed: 7806479]

Pang XD, and Guinan JJ, Jr. (1997). Effects of stapedius muscle contractions on the masking of auditory nerve responses. J. Acoust. Soc. Am 107, 3576–86.

Passchier-Vermeer W (1974). Hearing loss due to continuous exposure to steady-state broad-band noise. J. Acoust. Soc. Am 56, 1585–93. [PubMed: 4427029]

Rajan R, and Cainer KE (2008). Ageing without hearing loss or cognitive impairment causes a decrease in speech intelligibility only in informational maskers. Neuroscience, 154, 784–95. [PubMed: 18485606]

Rasmussen GL (1946). The olivary peduncle and other fiber projections of the superior olivary complex. J. Comp. Neurol 84, 141–219. [PubMed: 20982804]

Rasmussen GL (1953). Further observations of the efferent cochlear bundle. J. Comp. Neurol 99, 61–74. [PubMed: 13084783]

Rhode WS (1978). Some observation on cochlear mechanics. J. Acoust. Soc. Am 64, 158–76. [PubMed: 101571]

Rouiller EM, Capt M, Dolivo M, De Ribaupierre F (1989). Neuronal organization of the stapedius reflex pathways in the rat: a retrograde HRP and viral transneuronal tracing study. Brain Research, 476, 21–28 [PubMed: 2464420]

Ruan Q, Ao H, He J, Chen Z, Yu Z, Zhang R, Wang J,Yin S (2014). Topographic and quantitative evaluation of gentamicin induced damage to peripheral innervation of mouse cochlea. Neurotoxicol. 40, 86–96.

Salomon G (1963). Electromyography of middle ear muscles in man during motor activities. Acta Neurologica Scandinavica, 39, 161–8. [PubMed: 13991171]

Schairer KS, Feeney MP, Sanford CA (2013). Acoustic reflex measurement. Ear Hear. 34, Suppl. 1, 43–7.

Schmiedt RA, Mills JH, Boettcher FA (1996). Age-related loss of activity of auditory-nerve fibers. J. Neurophysiol 76, 2799–803. [PubMed: 8899648]

Sun XM (2008). Contralateral suppression of distortion product otoacoustic emissions and the middle-ear muscle reflex in human ears. Hear. Res 237, 66–75. [PubMed: 18258398]

Taberner AM, and Liberman MC (2005). Response properties of single auditory nerve fibers in the mouse. J. Neurophysiol 93, 557–69. [PubMed: 15456804]

Valero MD, Hancock KE, Liberman MC (2016). The middle-ear muscle reflex in the diagnosis of cochlear synaptopathy. Hear. Res 332, 29–38. [PubMed: 26657094]

Valero MD, Burton JA, Hauser S, Hackett T, Ramachandran R, Liberman MC (2017). Noise-induced cochlear synaptopathy in rhesus monkeys (Macaca mulatta). Hear. Res In press

Valero MD, Burton J, Hauser S, Hackett T, Ramachandran R, and Liberman MC (2017b). Cochlear synapatopathy in the noise-exposed and aging rhesus monkey (Macaca mulatta) Association for Research in Otolaryngology. Feb 11–15. Baltimore, MD

van den Berghe H, Kingma H, Kluge C, Marres EH (1990). Electrophysiological aspects of the middle ear muscle reflex in the rat: latency, rise time and effect on sound transmission. Hear Res 48, 209–19. [PubMed: 2272930]

Versnel H, Prijs VF, Schoonhoven R (1990). Single-fibre responses to clicks in relationship to the compound action potential in the guinea pig. Hear Res 46, 147–60. [PubMed: 2380121]

Vetter DE, Liberman MC, Mann J, Barhanin J, Boulter J, Brown MC, Saffiote-Kolman J, Heinemann SF, Elghoyen AB (1999). Role of alpha9 nicotinic Ach receptor subunits in the development and function of cochlear efferent innervation. Neuron, 23, 93–103. [PubMed: 10402196]

Viana LM, O'Malley JT, Burgess BJ, Jones DD, Oliviera CACP, Santos F, Merchant SN, Liberman LD, Liberman MC (2015). Cochlear neuropathy in human presbycusis: confocal analysis of hidden hearing loss in post-mortem tissue. Hear. Res 327, 78–88. [PubMed: 26002688]

Wang Y, and Ren C (2012). Effects of repeated "benign" noise exposures in young CBA mice: shedding light on age-related hearing loss. J. Assoc. Res. Otolaryngol 13, 505–515. [PubMed: 22532192]

Xu Y, Cheatham MA, Siegel JH (2017). Identifying the Origin of Effects of Contralateral Noise on Transient Evoked Otoacoustic Emissions in Unanesthetized Mice. J. Assoc. Res. Otolaryngol 18, 543–53. [PubMed: 28303411]

Zhao W, and Dhar S (2010). The effect of contralateral acoustic stimulation on spontaneous otoacoustic emissions. J. Assoc. Res. Otolaryngol 11, 53–67. [PubMed: 19798532]

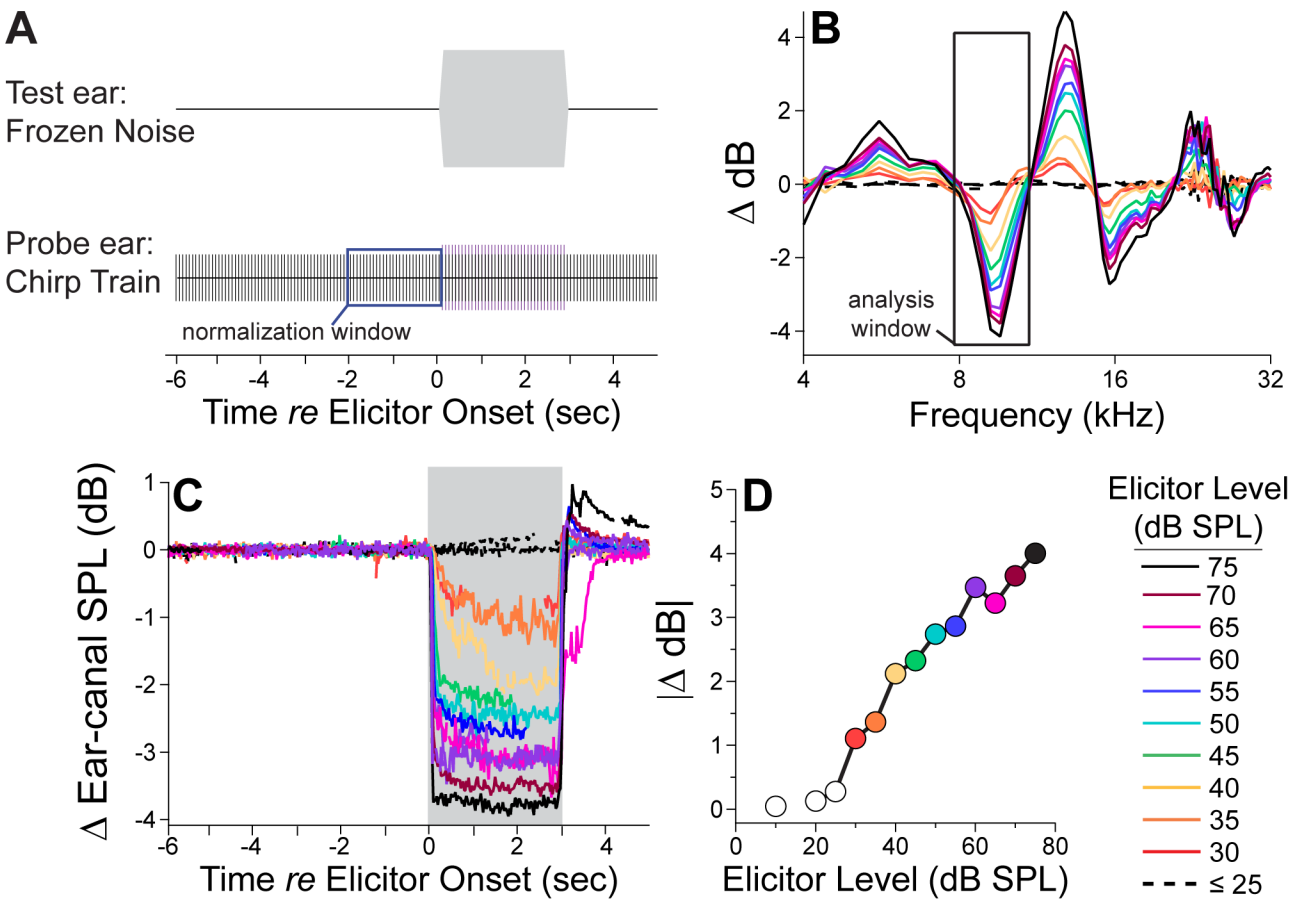

Figure 1. Measuring the wideband MEMR.

A: This stimulus schematic shows that the ipsilateral probe stimulus was a 40-Hz train of 2-msec "chirps" (70 or 80 dB SPL), upswept from 4 to 32 kHz, while the reflex elicitor was a 3-sec "frozen" noise (100-ms ramp), presented in alternating polarity every 11 sec to the contralateral ear. **B**: The ear-canal sound-pressure waveform of each chirp was measured and fast-Fourier transformed. The resultant spectra were averaged: one for the chirps within 2 secs before elicitor onset, and a second for the chirps during elicitor presentation. The difference between the two spectra was computed at the full range of elicitor levels (see key in **D**), and the analysis window (black box) centered on the first negative peak, where the "MEMR magnitude" was typically largest. **C**: The MEMR magnitude was computed in the time-domain by extracting the peak | Δ dB| within the analysis window for each chirp-evoked spectrum, before during and after the contralateral elicitor. **D**: To collapse the data to a single value at each elicitor level, we found the three-point time window during elicitor on-time that maximized | Δ dB|. Then, within this time window, we found the three consecutive frequency bins within the original frequency band that maximized | Δ dB|.

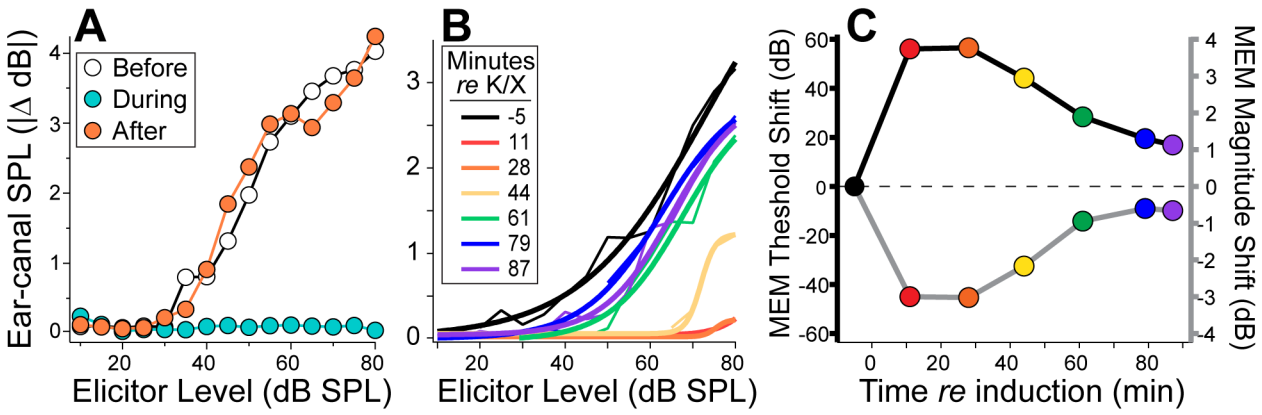

Figure 2. Sensitivity of MEMR to anesthesia.

A: MEMR growth functions from a single session, before (open), during (cyan), and after recovery from (orange) isoflurane anesthesia. **B**: MEMR growth functions from a different mouse from a single session before (black) and following injection of ketamine/xylazine anesthesia. Thick traces represent sigmoid fits to the measured data (thin traces). **C**: MEMR thresholds (black line, left axis) and magnitudes (gray line, right axis) extracted from the traces in **B** and normalized to the first measurement, taken 5 min prior to injection. Threshold was defined here as the elicitor level required to produce a | Δ dB| of 0.2; magnitude is the | Δ dB| for an elicitor at 80 dB SPL. Both subjects were α9 knockout mice. Elicitors were 4-octave-band noise (4-64 kHz).

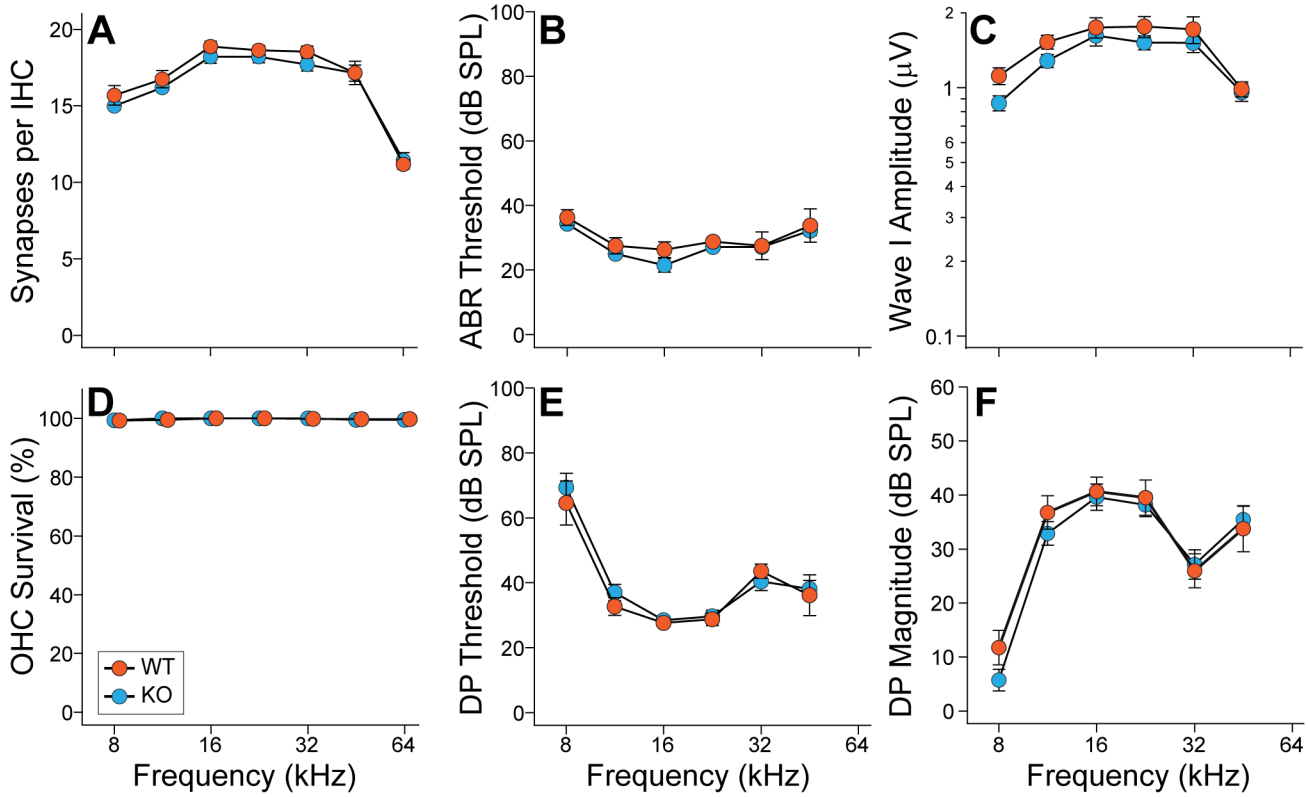

Figure 3. Cochlear histology and function were similar in WT and KO mice.

A: IHC synapse counts from the left ears 7 KO and 8 WT mice (from 20 adjacent IHCs in each cochlear location). **B,C:** ABR thresholds and suprathreshold wave-I amplitudes (at 70–80 dB SPL) were measured in all KO ears and a randomly selected half of the WT ears from **A**. **D:** OHC survival for the same ears as in **A** (data extracted from a 148-mm segment of the organ of Corti at each cochlear location in each ear). **E,F:** DPOAE thresholds and suprathreshold magnitudes (at 70–80 dB SPL) for the same ears as in **B** and **C**. Data are means ±1SEM. Symbol key in **D** applies to all panels.

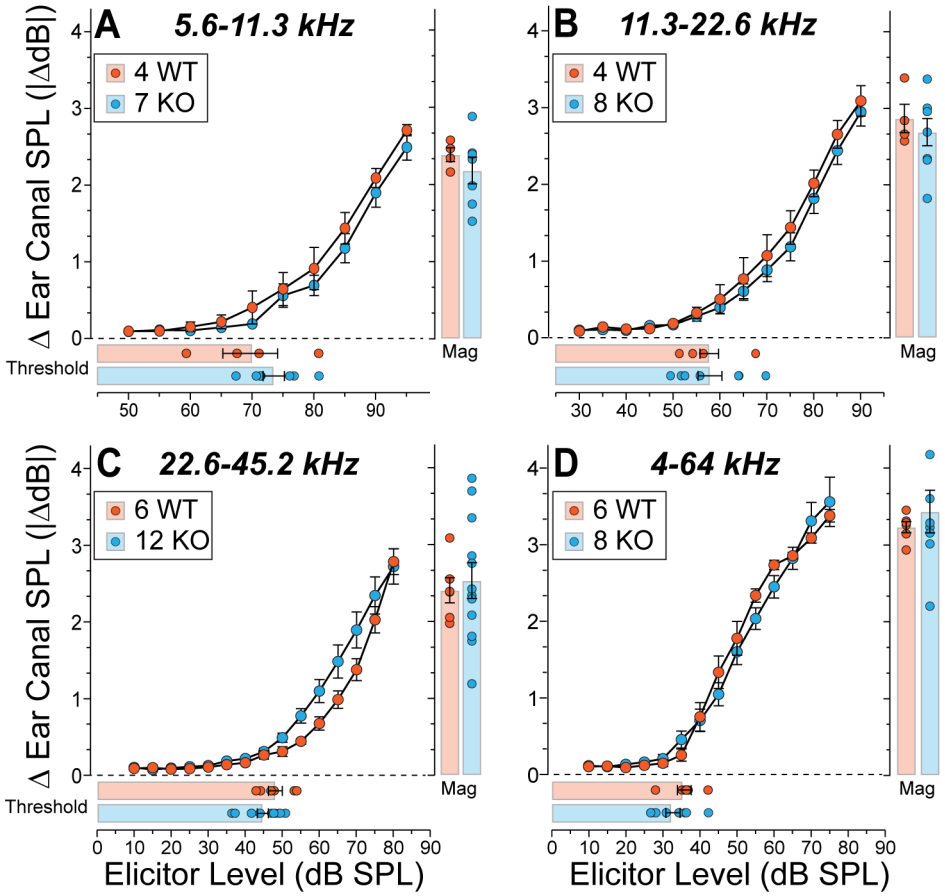

Figure 4. MEMR thresholds and magnitudes were similar in WT and KO mice.

Data are shown for four different elicitor bandwidths, as indicated in the panel header. Each panel shows the mean growth functions (±1SEM) for the MEMR, as well as individual threshold values and group means (±1SEM) below the x axis, and individual magnitude values (averaged over the highest two elicitor levels) and group means (±1SEM) at the right.

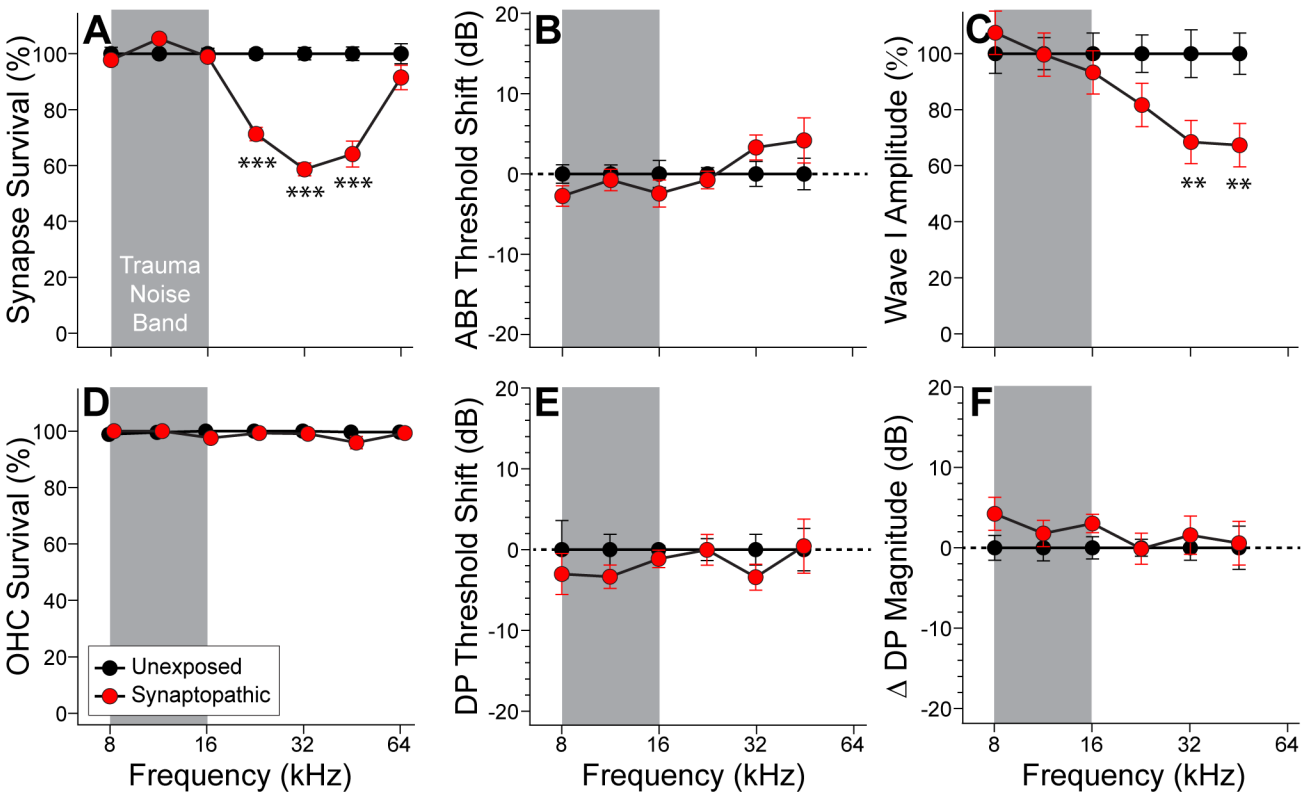

Figure 5. Noise exposure can produce cochlear synaptopathy with minimal permanent threshold shift.

A,D: Mean survival of IHC synapses and OHCs. **B,E:** Mean threshold shifts as measured by ABRs or DPOAEs, at 2 wks post-exposure. **C,F:** Mean suprathreshold amplitudes for ABR wave I and DPOAEs, respectively. In each ear, for each measure, response amplitudes were averaged across stimulus levels of 70–80 dB SPL. Values in all panels combine WT (2 unexposed, n= 8 synaptopathic) and KO (n= 7 unexposed, 6 synaptopathic) ears, as there were no clear differences between genotypes, and are normalized to means (±1 SEM) for unexposed, age-matched controls. Symbol key in **D** applies to all panels. Two noise-exposed WT mice showed no synaptopathy and were not included in these means. Asterisks indicate statistical significance by 1-way ANOVA: ** for P<.01; *** for P<.001.

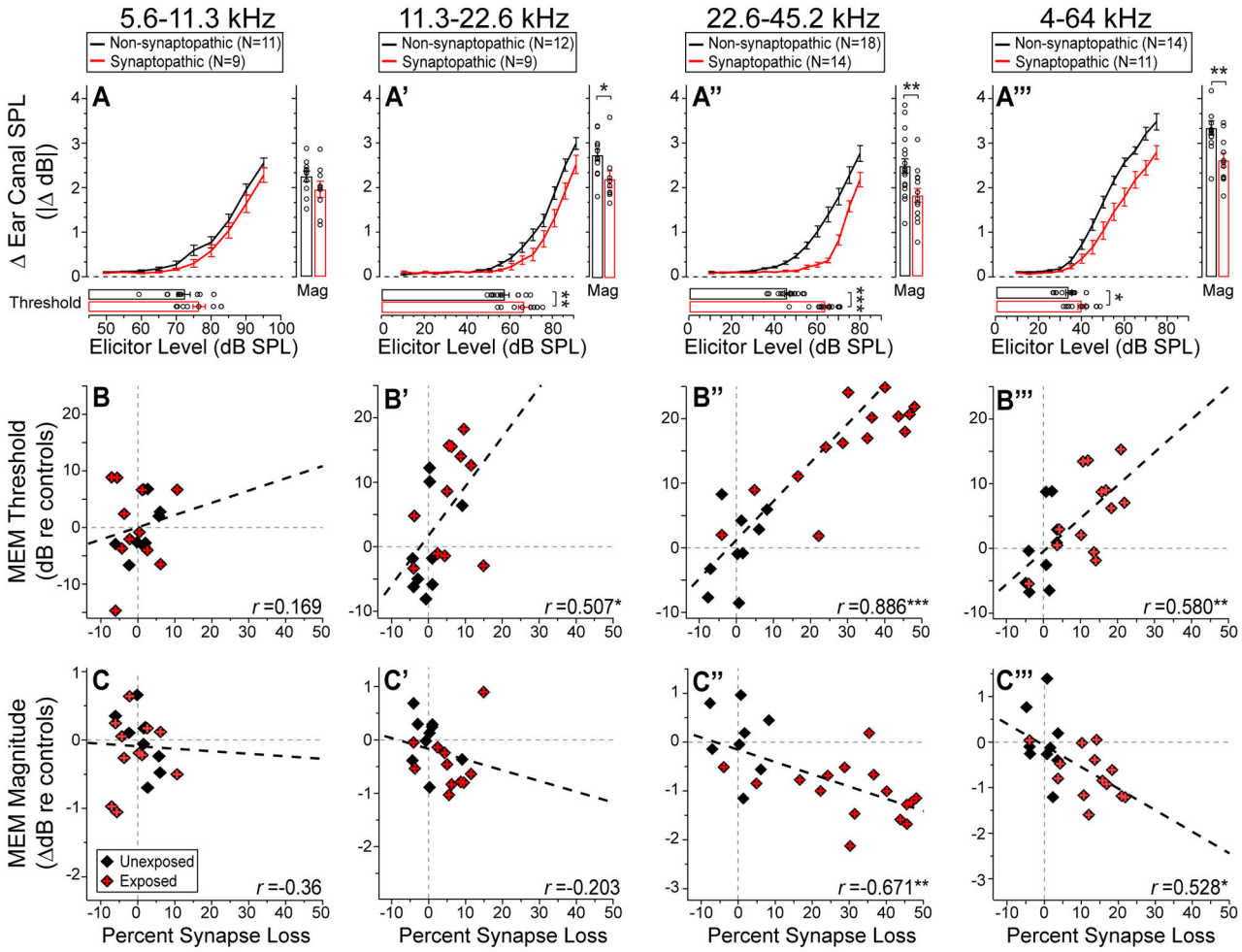

Figure 6. MEMRs were attenuated when the elicitor bandwidth spanned synaptopathic cochlear regions.

A-A’’’: Mean MEMR growth functions (±1 SEM) for four reflex elicitors, along with MEMR thresholds and magnitudes, displayed as in Figure 4. Comparisons are between synaptopathic and non-synaptopathic mice, with the latter group including all unexposed mice and two noise-exposed WT mice with no resultant synaptopathy. **B-B’’’:** MEMR thresholds, normalized to control means, plotted vs. the normalized synapse counts within the cochlear frequency region matching the elicitor passband. **C-C’’’:** MEMR maximum magnitude, normalized and plotted as in **B-B’’’**. For direct comparison, correlation coefficients for ABR wave-1 amplitude vs. synapse-loss (each averaged over the elicitor band width) was: r = 0.37, 0.24, and 0.56 for the octave-bands centered at 8, 16, and 32 kHz, respectively. Group sizes are given in panels **A-A’’’** - histology was not available for all unexposed mice undergoing reflex testing, and such mice were excluded from these panels. Asterisks indicate statistical significance: * for P<.05; ** for P<.01; *** for P<.001

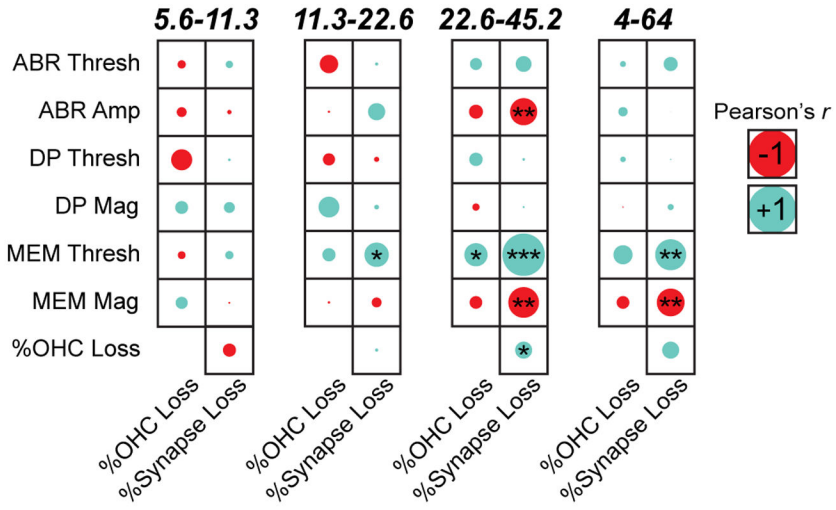

Figure 7. Synapse loss was best correlated with MEMR metrics.

Pearson correlation-coefficient matrices are shown for each physiologic metric vs. histologic metric. ABR, DPOAE and histological metrics were averaged over the frequency regions above each panel, which match the three octave-band (**A-C**) and the one broadband (**D**) MEM reflex elicitors. The diameter of each dot scales with Pearson's *r*, and each box width and height equal *r*=1. Red indicates a negative correlation and cyan represents a positive correlation. Asterisks indicate statistical significance (2-tailed): * for P<.05; ** for P<.01; *** for P<.001.